Geol. Mag. **145** (*3*), *2008, pp. 373–388.* © *2008 Cambridge University Press*
doi:10.1017/S0016756808004524 *Printed in the United Kingdom*

Longevity of the Permian Emeishan mantle plume (SW China): 1 Ma, 8 Ma or 18 Ma?

J. GREGORY SHELLNUTT*§, MEI-FU ZHOU*, DAN-PING YAN† & YANBIN WANG‡

*Department of Earth Sciences, The University of Hong Kong, Pokfulam Road, Hong Kong SAR, China
†State Key Laboratory of Geo-Processes and Mineral Resources, School of Earth Sciences and Resources, China University of Geosciences, Beijing, China
‡Beijing SHRIMP Center, Institute of Geology, Chinese Academy of Geological Science, Beijing, China

(*Received* 20 January 2007; *accepted* 26 July 2007; First published online 7 March 2008)

Abstract – After the formation of the ∼260 Ma Emeishan large igneous province, there were two volumetrically minor magmatic pulses at ∼252 Ma and ∼242 Ma, respectively. Alkaline mafic dykes intruding both 260 Ma and 252 Ma felsic plutons in the Panxi region, southwestern China, have compositions similar to the Emeishan flood basalts. One dyke is dated using the SHRIMP zircon U–Pb technique at 242 ± 2 Ma, ∼18 Ma younger than the start of Emeishan magmatism. The dykes have enriched light rare earth element patterns (La/YbN = 4.4–18.8) and trace element patterns similar to the Emeishan flood basalts and average ocean-island basalts. Some trace element ratios of the dykes (Zr/Nb = 3.8–8.2, La/Nb = 0.4–1.7, Ba/La = 7.5–25.6) are somewhat similar to EM1 source material, however, there are differences. Their εNd values (εNd = +2.6 and +2.7) and $_{I}$Sr ($_{I}$Sr = 0.704542 and 0.704554) ratios are indicative of a mantle source. Thus Emeishan magmatism may have lasted for almost 20 Ma after the initial eruption. However, geological evidence precludes the possibility that the post-260 Ma magmatic events were directly related to Emeishan magmatism, which began at and ended shortly after 260 Ma. The 252 Ma plutons and 242 Ma dykes represent volumetrically minor melting of the fossil Emeishan plume-head beneath the Yangtze crust. The 252 Ma magmatic event was likely caused by post-flood basalt extension of the Yangtze crust, whereas the 242 Ma event was caused by decompressional melting associated with the collision between the South China and North China blocks during the Middle Triassic.

Keywords: Emeishan large igneous province, mafic dykes, Middle Triassic, Late Permian, Middle Permian.

1. Introduction

Hotspot and mantle plume-related magmatism can vary in duration from tens of millions of years to less than one Ma (e.g. Richards, Duncan & Courtillot, 1989; Coffin & Eldholm, 1994; White & McKenzie, 1995). Some mantle plume-derived large igneous provinces have punctuated periods of magmatism while others have sustained periods of magmatism, and still others have a complete cessation of magmatism after the initial emplacement (e.g. Hooper, 1997; Courtillot *et al.* 1999; Ernst, Buchan & Campbell, 2005). Magmatism within a large igneous province will be sustained, providing that there is plentiful material to melt and the anomalous thermal conditions are maintained (e.g. White & McKenzie, 1989; Campbell & Griffiths, 1990).

The mantle plume-derived Emeishan large igneous province (ELIP) of southwestern China was emplaced at ∼260 Ma and consists of voluminous flood basalts and numerous ore-bearing mafic intrusions and associated felsic plutons (Zhou *et al.* 2002*a*; Ali *et al.* 2005). The age of the Emeishan large igneous province is controversial. The flood basalts have ^{40}Ar–^{39}Ar ages ranging from ∼251 Ma to ∼255 Ma while the plutonic rocks have U–Pb zircon ages of ∼260 Ma (Lo *et al.* 2002; Boven *et al.* 2002; Zhou *et al.* 2002*a*, 2005, 2006; Fan *et al.* 2004; Guo *et al.* 2004; Zhong & Zhu, 2006). However, Ali *et al.* (2004, 2005) have scrutinized the ^{40}Ar–^{39}Ar dates and suggest that the younger ages may have resulted from overprinting of the ^{40}K–^{40}Ar system during periods of tectonism in south China from the Permian to the Tertiary. Also, ^{40}Ar–^{39}Ar dates will yield slightly younger ages due to problems with the K-decay constant (Begemann *et al.* 2001). It has been suggested that the Emeishan large igneous province had a short duration of magmatism with nearly all volcanic and plutonic magmas emplaced within 1 Ma (Huang & Opdyke, 1998; Thompson *et al.* 2001; He *et al.* 2003, 2007). Recent studies have suggested that there was another period of magmatism in the same region at ∼252 Ma (Shellnutt & Zhou, 2006; Zhong *et al.* 2007). The younger period of magmatism implies that Emeishan-related magmatism was not continuous and was punctuated by magmatic episodes ∼8–9 Ma apart. The cause for the Late

§Author for correspondence: jgshelln@earth.sinica.edu.tw

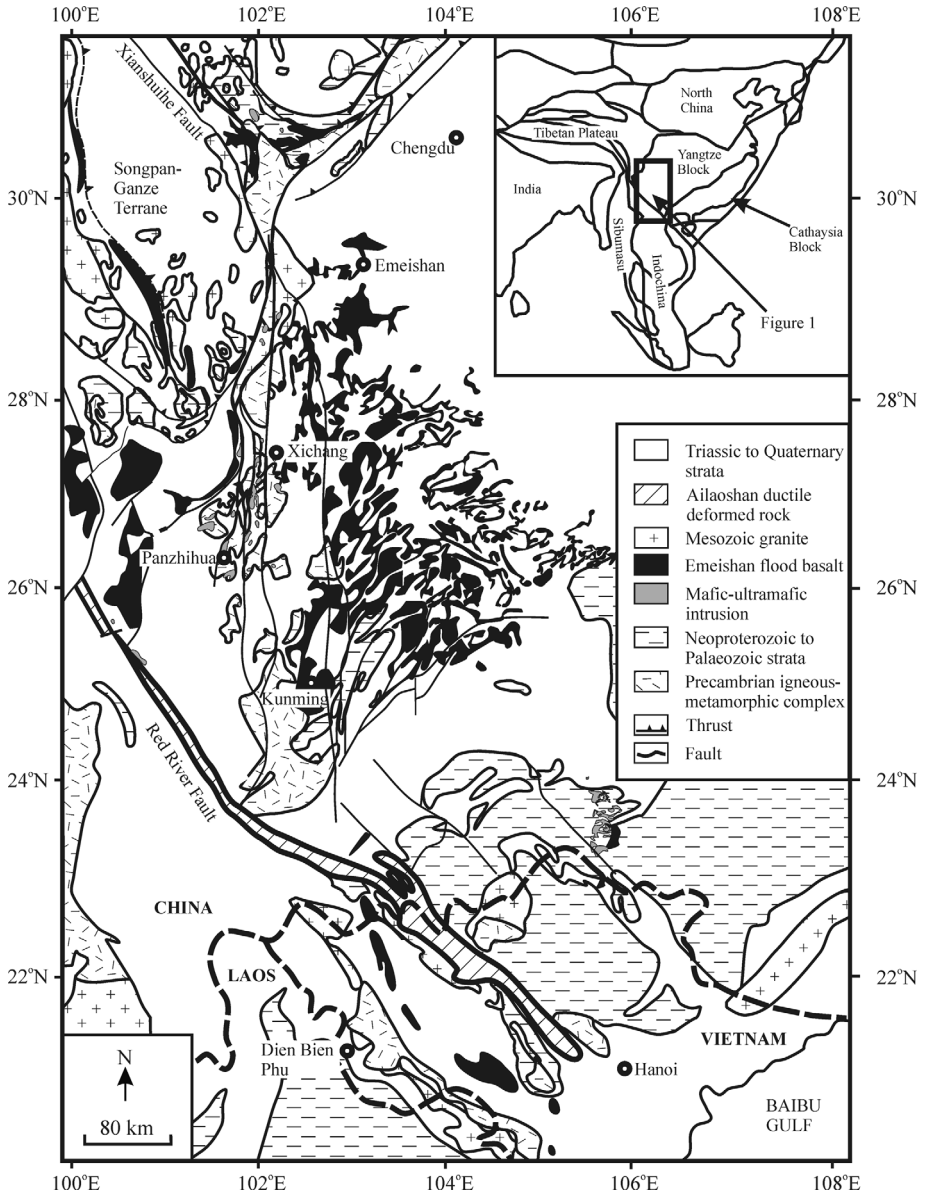

Figure 1. Regional geological map of the Emeishan large igneous province (modified from Zhou *et al.* 2002*b*).

Permian melting event is unknown, however, it is likely that post-260 Ma extension of the crust was responsible for the magmatism.

Mafic dykes represent periods of tensional magmatism that can be used to reconstruct palaeo-continents and examine the plumbing system of large igneous provinces (e.g. Halls, 1982; Pollard, 1987; Fahrig, 1987). In this paper we report mafic dykes that cross-cut Middle and Late Permian felsic and mafic intrusions of the Emeishan large igneous province. Our new SHRIMP zircon dating reveals that these dykes represent another post-ELIP magmatic event at ~ 242 Ma. To date, these dykes have been ignored in the literature. In this paper, we present SHRIMP zircon U–Pb ages, major and trace element analyses, and Nd–Sr isotopic analyses to determine the age and petrogenesis of the mafic dykes and their relationship to the Middle Triassic (~ 230 Ma) collision of the North and South China blocks.

2. Geological background

2.a. Regional geology

Southwestern China comprises the western margin of the Yangtze block to the east and the easternmost part of the Tibetan Plateau to the west (Fig. 1). The Yangtze block consists of Mesoproterozoic granitic gneisses and metasedimentry rocks that have been intruded by Neoproterozoic (~ 800 Ma) granites (Zhou *et al.* 2002*b*). The granites are overlain by a series of marine and terrestrial strata deposited from the Late Neoproterozoic (~ 600 Ma) to the Permian. The eastern part of the Tibetan Plateau is the

Songpan–Ganze terrane, a Late Triassic–Early Jurassic thrust sequence composed of 10 km thick marine sediments known as the Xikang Group (Bruguier, Lancelot & Malavieille, 1997; Yan *et al.* 2003*a*).

The South China block consists of the Cathaysia and Yangtze blocks, which collided during Neoproterozoic times (~ 1000 Ma) and may have been part of the Rodinian supercontinent (Li, Zhang & Powell, 1995; Yan *et al.* 2003*b*, 2006). The South China Block was situated along the margin of Gondwana from Cambrian to Silurian times and eventually rifted off during the Carboniferous and moved northward (Metcalfe, 2006). A low near-equatorial latitude is postulated for the South China block during the Permian because tropical to subtropical faunas with no Gondwanan affinities are found (Metcalfe, 2006).

Following northward movement, the Indochina block collided with the south margin of the South China block. The timing of collision, also known as the Indosinian tectonothermal event, between the two blocks remains controversial but was likely during Late Permian–Early Triassic times as recorded by metamorphic and igneous rocks (Nam, 1998; Meng & Zhang, 1999; Carter *et al.* 2001; Lepvrier *et al.* 2004; Yan *et al.* 2006). As a result, back-arc extension may have occurred in the South China block and produced a small volume of volcanic rocks. Continued northward drifting of the South China block eventually resulted in collision with the North China block during the Triassic, at ~ 230 Ma, creating the Qingling–Dabie–Sulu ultra-high pressure belt (Li *et al.* 1993).

2.b. Outline of the Emeishan large igneous province

The largest single geological feature of southwestern China is the Middle–Late Permian Emeishan large igneous province located along the western edge of the Yangtze Block near the boundary with the Songpan–Ganze terrane (Fig. 1). The distribution of the Emeishan large igneous province was subsequently affected in the Mesozoic and Cenozoic by post-emplacement faulting associated with the development of the Songpan–Ganze terrane and the Indo-Eurasian collision (Chung & Jahn, 1995). The Emeishan large igneous province covers an area of 0.3×10^6 km^2 within southwestern China and northern Vietnam and consists of flood basalts, spatially associated felsic plutons and layered mafic–ultramafic intrusions, some of which host giant Fe–Ti–V oxide deposits (e.g. Zhong *et al.* 2002; Zhou *et al.* 2005). The volcanic succession includes picrites, basaltic andesites and basalts that are subdivided on the basis of TiO_2 into high- and low-Ti/Y groups (Xu *et al.* 2001; Song *et al.* 2001). The basalt piles range in thickness from 1.0 to 5.0 km in the western part and 0.2 to 2.6 km in the eastern part. A mantle plume model is used to explain the geological features such as the extensive flood basalts, ultramafic lavas, short-duration, structural doming and lower crustal seismic velocity layers (Chung *et al.* 1998; He *et al.* 2003; Xu *et al.* 2004).

3. Field relations and petrography of the mafic dykes

In the Panxi region, between the cities of Panzhihua and Xichang (Fig. 1), there are abundant felsic and mafic plutonic rocks. Intruding these plutons are narrow (generally ≤ 5 m wide) mafic dykes. These dykes have variable strikes of 306°, 185° and 85°; most have steep E to SE dips of 70–90° (Fig. 2). In some instances the dykes may be responsible for recrystallization of their hosts because they are parallel to recrystallization fabrics. The dykes are relatively easy to spot because of their colour contrast with that of their felsic hosts. However, they are seen intruding mafic intrusions as well. Due to their limited volume and exposure, it may be inappropriate to identify them as a dyke swarm until more systematic mapping reveals their total extent. For this study, dykes intruding the ~ 260 Ma Baima, ~ 260 Ma Woshui and ~ 252 Ma Huangcao plutons were sampled to determine if they are related to Emeishan magmatism (Fig. 2). One coarse-grained dyke intruding the Baima pluton was sampled for radiometric age dating and samples of this dyke and the other dykes were analysed for bulk rock compositions.

The mafic dykes show variable textures, with most being aphanitic, however, there are medium-grained varieties with ophitic to sub-ophitic textures. The dykes consist primarily of plagioclase (50 %), clinopyroxene (35 %), biotite (5–10 %), and Fe–Ti oxides (5–10 %), with minor amounts of olivine (< 5 %), apatite (< 5 %) and sulphides. Alteration of clinopyroxene to hornblende is common, and there are many cases of biotite forming an alteration rim around magnetite. The dykes differ considerably from other mafic intrusions of the Panxi region because they have diabasic textures, while the other mafic intrusions are granular and have cumulate textures.

4. Analytical methods

4.a. SHRIMP zircon analyses

Zircon crystals were separated from a sample (GS04-119) of one dyke (dyke 2) using conventional heavy liquid and magnetic techniques, mounted in epoxy, polished, coated with gold, and photographed in transmitted and reflected light to identify grains for analysis. U–Pb isotopic ratios of zircon crystals were measured from a single spot of each mineral using the SHRIMP II at the Chinese Academy of Geological Sciences, Beijing, China. The measured isotopic ratios were reduced off-line using standard techniques (see Claoué-Long *et al.* 1995) and the U–Pb ages were normalized to a value of 417 Ma determined by conventional U–Pb analysis of zircon standard TEMORA 1 (Black *et al.* 2003*a*,*b*). Common Pb was

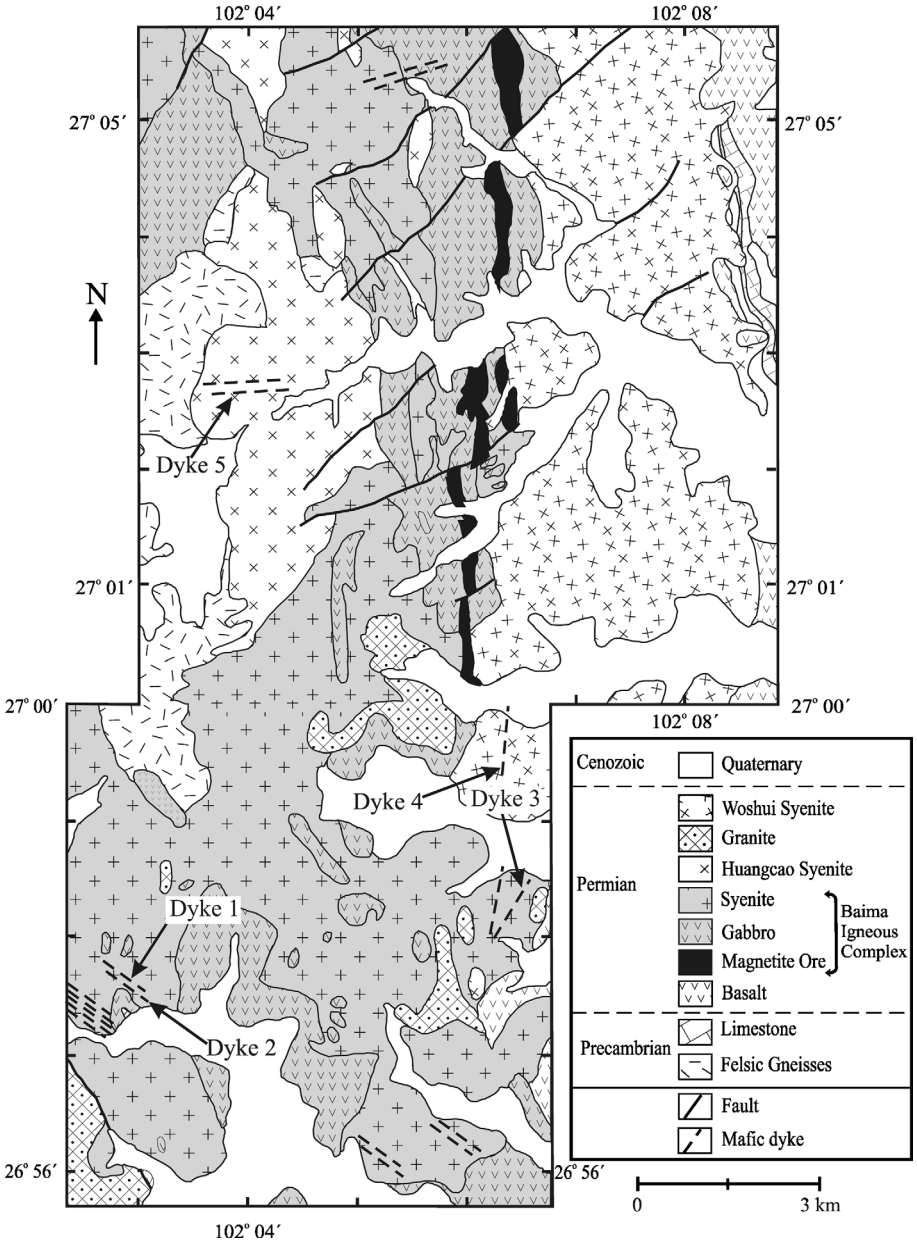

Figure 2. Local geological map of the Baima region showing the distribution and sampling locations of the mafic dykes (modified from Wang *et al.* 1994 and Xiong *et al.* 1996).

corrected using the methods of Compston, Williams & Meyer (1984). The $^{206}Pb/^{238}U$ and $^{207}Pb/^{235}U$ data were adjusted for systematic bias in the measurements of the TEMORA 1 standard.

4.b. Major and trace elemental analyses

Major elements were analysed by X-ray fluorescence spectroscopy at the University of Hong Kong using glass discs (Gill, 1997). Trace elements were analysed by inductively coupled plasma mass spectrometry (ICP-MS) using the technique of Qi, Jing & Gregoire (2000), also at the University of Hong Kong. Standard reference materials for the major elements were BHVO-2, JGB-2 and GXR-1. For the trace element analysis, the standard reference materials were AMH-1 and GBPG-1 (Thompson *et al.* 1999; Potts *et al.* 2000, 2001). The precisions for the major and trace element results are better than 5 % and 10 %, respectively.

4.c. Rb–Sr and Sm–Nd isotopic analyses

Isotopic ratios were measured using a Finnigan MAT-262 thermal ionization mass spectrometer in the Laboratory for Radiogenic Isotope Geochemistry, Institute of Geology and Geophysics, Chinese Academy of Sciences, Beijing. The raw data were processed using the Isoplot program which gave the 2σ error (Ludwig, 2001). $^{143}Nd/^{144}Nd$ ratios were normalized to $^{146}Nd/^{144}Nd = 0.7219$ and $^{87}Sr/^{86}Sr$ ratios to

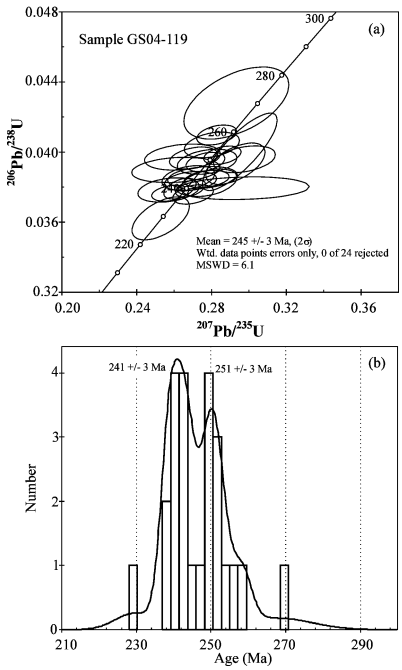

Figure 3. (a) Concordia diagram of the SHRIMP zircon U/Pb dating results for sample GS04-119. (b) Gaussian distribution profile of the ages yielded from individual zircon crystals.

$^{86}Sr/^{88}Sr = 0.1194$. Details of analytical procedures are described in Chen, Hegner & Todt (2000) and Chen *et al.* (2002). The USGS reference material used was BCR-1, which is indistinguishable from the updated reference material BCR-2 (Raczek, Jochum & Hofmann, 2003).

5. Results

5.a. SHRIMP zircon U–Pb dating

Zircon grains from sample GS04-119 have both euhedral and anhedral shapes and are subdivided into two populations based on smaller ($\leq 150\ \mu$m) and larger grain size ($> 150\ \mu$m). Their Th/U ratios vary from 0.21 to 0.58 with an average of 0.37 and standard deviation of 0.08 (Table 1). All individual zircon data were plotted on a concordia diagram and yield an age of 245 ± 3 Ma with a high mean square of weighted deviates (MSWD) of 6.1 (Fig. 3a). Both grain sizes produced nearly identical ages, with the smaller grains yielding an age of 243 ± 5 Ma and the larger grains yielding an age of 246 ± 4 Ma; however, their MSWD are still very high at 5.6 and 6.4, respectively. The cumulative Gaussian distribution profile shows clusters of $^{206}U/^{238}Pb$ mean ages at 241 ± 3 Ma and 251 ± 3 Ma (Fig. 3b). We interpret the age of the dyke to be 242 ± 2 Ma (MSWD of 0.75) because dykes of similar composition to sample GS04-119 cut the 252 Ma Huangcao pluton, therefore they likely represent the younger ages. The ~ 250 Ma age cluster shown in the distribution profile is not likely the intrusion age because it would be highly improbable that a dyke would contain a majority of zircons younger than its emplacement age.

5.b. Whole rock geochemistry

The five mafic dykes sampled have evolved mafic compositions, with Mg no. ($100 \times (Mg^{2+}/(Mg^{2+}+Fe^{2+}))$) ranging from 37.8 to 60.2 (Table 2). The rocks are alkaline in composition ($Na_2O+K_2O = 3.96$–6.75 wt %) and contain variable SiO_2 (44.6–53.5 wt %), Fe_2O_3t (11.3–17.9 wt %; t = total Fe expressed as Fe^{3+}), MgO (3.5–6.5 wt %), CaO (6.2–11.7 wt %) and P_2O_5 (0.2–1.2 wt %) (Fig. 4). The negative correlations of Fe and Ca, and positive trends of Al, K and Na against Si, strongly suggest that these dykes were products of fractionation crystallization of a primitive parental magma (Fig. 4). Most of the samples were collected from dyke 1 which is ~ 25 metres wide. The dyke does not show chemical variation across (GS03-021-030) with the exception of samples GS03-117 and -118, which have the highest SiO_2 wt % and lowest MgO wt % content and are located near the northeastern contact with the Baima syenitic pluton.

The mafic dykes have highly variable concentrations of compatible trace elements, for example, Sc (15–35 ppm), Ni (17–87 ppm), Co (25–62 ppm), Cu (36–468 ppm), V (121–1121 ppm) and Cr (2–85 ppm). The trace element classification diagram of Winchester & Floyd (1977) shows the data are consistent with alkaline olivine basalts (Fig. 5). The dykes have rare earth element (REE) profiles enriched in light REE ($La/Yb = 4.4$–18.8) with a range of Eu/Eu^* ($Eu/Eu^* = 2^*Eu_N/(Sm_N+Gd_N)$) ratios (0.70–1.27) (Fig. 6). The primitive mantle-normalized incompatible trace element plots show a slight enrichment of the large-ion lithophile elements (LILE) (Cs, Rb, Ba), a negative Sr anomaly and a slight depression of Hf–Zr (Fig. 7). A slightly negative Hf–Zr anomaly is common in the intrusive mafic igneous rocks from the Emeishan large igneous province, however, it is not universal (Zhou *et al.* 2005, 2006; Zhang *et al.* 2006). The depletion in Hf–Zr could be related to previous extraction of mafic magmas from the same source.

Whole rock Sr and Nd isotope ratios were determined for two samples of dyke 1 (Table 3). The $\varepsilon Nd_{(t)}$ ratios and $(^{87}Sr/^{86}Sr)_i$ ratios have been age-corrected to 242 Ma. The samples from dyke 1 intrude the Baima pluton and are ~ 20 m apart. The $\varepsilon Nd_{(t)}$ values (+2.6 and +2.7), as well as their initial $^{87}Sr/^{86}Sr$ ratios (0.704542 and 0.704554), are similar to values of the Emeishan flood basalts and surrounding intrusions (Fig. 8).

6. Discussion

6.a. Petrogenesis of the 242 Ma dykes

The mafic dykes of the Panxi region are chemically and petrographically similar to alkaline olivine

Table 1. SHRIMP zircon U–Pb data of mafic dyke 2

Spot	Th/U	U (ppm)	Th (ppm)	$^{206}Pb_c$ (%)	$^{206}Pb^*$ (ppm)	(1) ^{206}Pb–^{238}U Age	(2) ^{206}Pb–^{238}U Age	(3) $^{206}Pb/^{238}U$ Age	(1) $^{208}Pb/^{232}Th$ Age	(1) ^{238}U–$^{206}Pb^*$	(1) $^{207}Pb^*/^{206}Pb^*$	(1) $^{207}Pb^*/^{235}U$	(1) $^{206}Pb^*/^{238}U$
GS04-119.1*	0.46	677	312	0.25	22.4	242.5 ± 2.2	242.6 ± 2.3	244.0 ± 2.4	234 ± 76	26.08 ± 0.94	0.0509 ± 3.3	0.2688 ± 3.4	0.0383 ± 0.94
GS04-119.2*	0.31	485	148	0.14	16.1	243.7 ± 2.9	243.9 ± 2.9	243.7 ± 3.0	213 ± 76	25.96 ± 1.2	0.0504 ± 3.3	0.2676 ± 3.5	0.0385 ± 1.2
GS04-119.3*	0.34	363	123	0.19	11.8	239.4 ± 2.9	239.9 ± 2.9	240 ± 3.1	161 ± 95	26.43 ± 1.2	0.0493 ± 4.0	0.2570 ± 4.2	0.0378 ± 1.2
GS04-119.4	0.33	492	163	0.26	16.8	250.7 ± 2.6	251.3 ± 2.6	251.4 ± 2.8	169 ± 69	25.22 ± 1.0	0.0494 ± 3.0	0.2704 ± 3.1	0.0397 ± 1.0
GS04-119.5	0.37	544	202	0	18.7	252.9 ± 9.1	252.2 ± 9.1	252.7 ± 9.6	350 ± 58	24.99 ± 3.7	0.0535 ± 2.6	0.2950 ± 4.5	0.0400 ± 3.7
GS04-119.6*	0.35	502	176	0.26	16.5	242.0 ± 3.2	241.5 ± 3.3	242.9 ± 3.4	321 ± 75	26.14 ± 1.4	0.0528 ± 3.3	0.2786 ± 3.6	0.0383 ± 1.4
GS04-119.7*	0.54	1061	578	0	34.6	239.9 ± 2.4	240.1 ± 2.5	240.4 ± 2.7	211 ± 44	26.38 ± 1.0	0.0503 ± 1.9	0.2631 ± 2.2	0.0379 ± 1.0
GS04-119.8	0.31	387	119	0.51	14.3	270.2 ± 8.4	270.8 ± 8.5	271.2 ± 8.9	181 ± 130	23.37 ± 3.2	0.0497 ± 5.5	0.2930 ± 6.3	0.0428 ± 3.2
GS04-119.9*	0.37	979	361	0.11	32.4	243.3 ± 2.0	242.9 ± 2.0	243.7 ± 2.1	299 ± 62	26.00 ± 0.84	0.0523 ± 2.7	0.2774 ± 2.9	0.0385 ± 0.84
GS04-119.10	0.35	798	276	0	27.3	251.7 ± 2.1	251.4 ± 2.2	251.2 ± 2.3	288 ± 49	25.12 ± 0.87	0.0521 ± 2.1	0.2858 ± 2.3	0.0398 ± 0.87
GS04-119.11	0.26	339	89	0.52	11.6	251.1 ± 3.1	252.0 ± 3.1	252.6 ± 3.2	115 ± 120	25.18 ± 1.2	0.0483 ± 4.9	0.2650 ± 5.1	0.0397 ± 1.2
GS04-119.12	0.21	690	147	0	24.3	258.9 ± 2.3	259.3 ± 2.4	258.7 ± 2.4	197 ± 54	24.41 ± 0.92	0.0501 ± 2.3	0.2828 ± 2.5	0.0410 ± 0.92
GS04-119.13	0.38	714	274	0	24.2	249.3 ± 2.2	249.4 ± 2.3	249.8 ± 2.4	236 ± 53	25.36 ± 0.91	0.0509 ± 2.3	0.2768 ± 2.5	0.0394 ± 0.91
GS04-119.14	0.58	1598	922	0.12	51.8	238.2 ± 1.9	238.6 ± 1.9	239.4 ± 2.2	180 ± 56	26.56 ± 0.80	0.0497 ± 2.4	0.2578 ± 2.5	0.0376 ± 0.80
GS04-119.15*	0.38	336	127	0.58	11.3	246.5 ± 3.0	247.3 ± 2.9	247.1 ± 3.1	127 ± 140	25.66 ± 1.2	0.0486 ± 5.8	0.2610 ± 6.0	0.0390 ± 1.2
GS04-119.1.1	0.35	417	147	0.14	14.5	255.3 ± 3.0	255.7 ± 3.0	256.3 ± 3.2	209 ± 76	24.75 ± 1.2	0.0503 ± 3.3	0.2802 ± 3.5	0.0404 ± 1.2
GS04-119.1.2	0.34	287	97	0	9.75	250.3 ± 3.1	249.3 ± 3.2	250.1 ± 3.3	393 ± 77	25.26 ± 1.3	0.0545 ± 3.4	0.2980 ± 3.7	0.0396 ± 1.3
GS04-119.1.3	0.28	378	106	0	12.8	248.7 ± 4.8	247.8 ± 4.9	248.8 ± 5.1	371 ± 67	25.42 ± 2.0	0.0540 ± 3.0	0.2930 ± 3.6	0.0393 ± 2.0
GS04-119.1.4	0.40	420	168	0	14.2	249.4 ± 2.9	249.4 ± 3.0	249.9 ± 3.2	243 ± 83	25.35 ± 1.2	0.0510 ± 3.6	0.2780 ± 3.8	0.0394 ± 1.2
GS04-119.1.5	0.34	638	214	0.15	19.9	229.3 ± 5.0	229.3 ± 5.1	229.7 ± 5.3	225 ± 77	27.62 ± 2.2	0.0506 ± 3.3	0.2530 ± 4.0	0.0362 ± 2.2
GS04-119.1.6	0.40	563	226	0	18.2	237.8 ± 2.3	237.5 ± 2.3	237.7 ± 2.5	292 ± 56	26.61 ± 0.97	0.0521 ± 2.5	0.2702 ± 2.7	0.0376 ± 0.97
GS04-119.1.7*	0.43	1159	493	0	37.8	240.0 ± 2.0	239.9 ± 2.1	241.1 ± 2.2	259 ± 41	26.36 ± 0.86	0.0514 ± 1.8	0.2688 ± 2.0	0.0379 ± 0.86
GS04-119.1.8*	0.37	507	189	2.19	16.9	240.1 ± 2.7	238.3 ± 2.4	239.0 ± 2.7	482 ± 170	26.36 ± 1.1	0.0568 ± 7.8	0.2970 ± 7.9	0.0379 ± 1.1
GS04-119.1.9*	0.40	440	175	0.36	14.6	243.8 ± 2.6	243.6 ± 2.6	244.0 ± 2.8	276 ± 99	25.95 ± 1.1	0.0518 ± 4.3	0.2750 ± 4.5	0.0385 ± 1.1

Errors are 1σ; Pb_c and Pb^* indicate the common and radiogenic portions, respectively. Error in standard calibration was 0.64% (not included in above errors but required when comparing data from different mounts). (1) Common Pb corrected using measured ^{204}Pb. (2) Common Pb corrected by assuming $^{206}Pb/^{238}U$–$^{207}Pb/^{235}U$ age-concordance. (3) Common Pb corrected by assuming $^{206}Pb/^{238}U$–$^{208}Pb/^{232}Th$ age-concordance. Populations of zircons > 150 μm listed as 119.1–119.15 and < 150 μm listed as 119.1.1–119.1.9. Samples which comprise the 242 Ma age are denoted by *

Table 2. Whole rock chemical analyses of the mafic dykes

Sample	GS04-021	GS04-023	GS04-024	GS04-025	GS04-026	GS04-028	GS04-029	GS04-030	GS04-117	GS04-118	GS04-119	GS03-105	GS03-106	GS03-111	GS03-115	GS03-124
Pluton	Baima	Baima	Baima	Baima	Baima	Baima	Baima	Baima	Baima	Baima	Baima	Baima	Baima	Woshui	Woshui	Huangcao
Dyke	Dyke-1	Dyke-1	Dyke-1	Dyke-1	Dyke-1	Dyke-1	Dyke-1	Dyke-1	Dyke-1	Dyke-1	Dyke-2	Dyke-3	Dyke-3	Dyke-4	Dyke-4	Dyke-5
SiO_2 (wt %)	46.35	46.09	45.43	44.6	45.01	44.86	46.19	45.5	48.41	51.86	44.76	46.15	47.43	46.72	47.08	53.51
TiO_2	4.87	3.11	3.88	4.38	3.97	4.13	2.03	4.99	3.12	1.95	4.95	3.86	3.76	2.8	2.62	1.74
Al_2O_3	12.16	11.55	12.9	11.36	12.42	12.1	14.49	11.49	13.15	14.4	11.56	14.15	14.43	12.83	13.27	16.01
Fe_2O_3t	17.86	15.96	16.13	17.91	16.48	17.04	13.15	17.54	15.35	11.3	17.9	13.84	13.37	15.76	14.64	9.2
MnO	0.26	0.32	0.22	0.24	0.24	0.24	0.21	0.26	0.29	0.19	0.29	0.22	0.2	0.25	0.24	0.14
MgO	5.48	6.41	5.71	6.43	5.89	6.23	6.12	5.43	4.86	5.13	5.65	4.66	4.36	5.29	5.77	3.51
CaO	10.16	9.72	10.48	10.64	10.16	10.48	11.13	9.44	8.95	8.98	9.46	8.48	8.04	9.85	10.47	6.18
Na_2O	2.83	3.32	3.18	2.62	3.23	2.93	3.63	3.24	3.87	4.37	3.03	4.02	4.06	3.34	3.62	3.72
K_2O	1.18	2.1	1.13	1.08	1.34	1.21	1.34	1.41	1.6	1.75	1.55	1.17	1.51	1.17	1.09	2.39
P_2O_5	0.49	0.33	0.27	0.27	0.3	0.28	0.34	0.35	0.47	0.24	0.35	0.86	0.92	0.67	0.61	0.7
LOI	−0.16	0.81	0.63	0.43	0.6	0.39	0.83	0.09	0.54	0.7	0.65	1.93	1.46	0.22	0.33	1.44
Total	101.48	99.7	99.94	99.95	99.64	99.89	99.46	99.75	100.6	100.86	100.15	99.36	99.55	98.92	99.76	98.54
Mg no.	37.8	44.3	41.2	41.6	41.5	42	48	38	38.5	47.3	38.5	40	39.3	40	43.9	43.1
Sc (ppm)	33	34	31	35	33	34	32	32	28	29	30	18	17	32	32	17
V	1070	694	857	970	893	916	458	1121				339	309	432	409	122
Cr	10	66	24	31	26	27	18	8	43	68	30	6	2	42	60	43
Co	55	53	55	62	57	60	48	56	45	39	57	41	37	47	46	25
Ni	53	77	56	69	61	62	49	44	56	55	64	29	21	54	59	28
Cu	468	155	294	394	333	327	215	444	173	51	376	42	45	115	102	37
Zn	155	239	145	157	158	143	179	156	199	137	200	142	141	156	140	116
Ga	23	22	22	22	23	22	18	23	26	21	24	25	25	21	21	21
Rb	36	168	47	40	62	53	59	51	95	139	82	27	48	29	26	55
Sr	386	326	425	357	401	398	563	397	399	355	405	1161	1140	419	416	583
Y	33	37	25	27	26	26	21	32	41	28	30	27	29	34	33	27
Zr	223	259	169	178	165	172	100	238	220	172	198	187	213	128	132	267
Nb	31	39	21	22	21	21	26	34	48	23	30	30	33	25	23	33
Cs	0.7	1.4	0.7	0.8	0.7	0.7	1.3	1.1	1.1	2.7	0.7	0.4	0.6	0.6	0.5	0.8
Ba	360	316	294	297	310	310	496	393	528	497	410	1074	1317	728	669	1014
La	33.7	38.1	23.4	23.6	24.5	23.9	28.3	30.9	39.9	30.3	29.0	44.1	46.1	28.9	26.9	55.4
Ce	74.8	82.7	51.9	52.7	54.2	53.3	58.1	68.2	91.9	62.3	69.3	99.6	105.9	61.6	57.8	103.9
Pr	9.8	10.5	6.7	7.1	7.2	7.0	7.0	8.9	11.4	7.3	8.9	13.5	14.4	7.9	7.5	11.5
Nd	42.1	42.3	29.0	30.6	30.5	30.5	28.2	38.0	46.2	28.9	35.7	59.5	61.9	34.0	31.9	43.3
Sm	9.1	9.2	6.6	6.9	6.8	6.8	5.5	8.3	9.9	6.0	8.0	11.9	12.1	7.1	6.7	7.4
Eu	2.7	2.5	2.2	2.2	2.2	2.2	1.9	2.6	3.0	1.6	2.5	4.8	5.0	2.7	2.7	2.6
Gd	8.0	7.9	5.6	6.0	6.0	5.9	4.8	7.3	7.9	5.0	6.4	11.0	11.5	7.7	7.1	8.0
Tb	1.4	1.4	1.0	1.0	1.0	1.1	0.8	1.3	1.4	0.9	1.1	1.4	1.5	1.2	1.1	1.1
Dy	7.1	7.7	5.2	5.6	5.5	5.6	4.3	6.7	8.1	5.5	6.4	6.4	6.6	6.2	5.9	5.2
Ho	1.3	1.5	1.0	1.1	1.0	1.1	0.8	1.3	1.6	1.1	1.3	1.1	1.2	1.3	1.2	1.0
Er	3.7	4.1	2.6	2.9	2.8	2.8	2.3	3.6	4.2	3.0	3.3	2.9	3.1	3.7	3.6	2.9
Tm	0.5	0.6	0.4	0.4	0.4	0.4	0.3	0.5	0.6	0.5	0.5	0.3	0.3	0.5	0.5	0.4
Yb	2.9	3.6	2.2	2.3	2.3	2.4	2.0	2.9	3.8	2.9	2.9	2.0	2.0	3.3	3.2	2.6
Lu	0.4	0.5	0.3	0.3	0.3	0.3	0.3	0.4	0.6	0.5	0.4	0.3	0.3	0.5	0.5	0.4
Hf	6.1	7.0	4.7	4.9	4.6	4.8	2.7	6.6	6.1	5.0	5.7	4.8	5.6	3.5	3.5	6.0
Ta	2.4	2.7	1.6	1.6	1.5	1.6	1.6	2.6	4.2	1.7	2.1	2.1	2.3	1.4	1.4	1.8
Th	4.3	6.4	3.1	3.2	3.2	3.1	3.3	5.0	5.1	9.1	3.9	3.3	3.6	4.0	3.8	7.0
U	1.0	1.4	0.8	0.8	0.8	0.8	0.8	1.2	1.3	1.9	1.0	0.9	1.0	0.9	0.9	1.3

Table 2. Continued.

Sample	GS04-021	BHVO-2	BHVO-2	JGB-2	JGB-2	GXR-1	GXR-1	GBPG-1	GBPG-1	AMH-1	AMH-1
Pluton	Duplicate	Standard	Standard	Standard	Standard	Standard	Standard	Standard	Standard	Standard	Standard
Dyke	Dyke-1	R.V.	measured	R.V.	measured	R.V.	measured	R.V.	this study	R.V.	this study
SiO_2 (wt.%)	45.56	49.75	49.90	48.34	46.68	48.83	48.57				
TiO_2	4.61	2.75	2.73	0.57	0.58	0.06	0.06				
Al_2O_3	11.84	13.66	13.50	24.82	23.32	6.83	6.64				
Fe_2O_3t	17.59	12.27	12.30	6.60	6.85	34.77	33.80				
MnO	0.26	0.17		0.13	0.13	0.13	0.11				
MgO	5.49	7.27	7.23	6.66	6.24	0.40	0.36				
CaO	9.98	11.67	11.40	14.82	14.20	1.25	1.34				
Na_2O	3.03	2.16	2.22	0.95	0.92	−0.02	0.07				
K_2O	1.23	0.58	0.52	−0.08	0.06	0.05	0.06				
P_2O_5	0.48	0.27	0.27	0.02	0.01	0.15	0.15				
LOI	−0.10	−0.40	−0.40			4.99	4.99				
Total	99.96	100.14	99.67	102.83	98.98	97.44	96.15				
Mg no.											
Sc (ppm)								13.93	17.24	13.48	14.99
V								96.5	95.7	106.4	106.4
Cr								181.4	180.5	40.89	41.5
Co								19.5	19.9	18.68	18.9
Ni								59.6	58.8	32.36	35.1
Cu								30.0	31.8	30.2	32.7
Zn								80.3	72.4	66.9	64.5
Ga								18.6	20.0	20.49	20.2
Rb								56.2	56.2	18.31	18.2
Sr								363.5	366.0	545.4	550.9
Y								18.0	17.3	16.44	14.86
Zr								231.8	226.1	146	144.2
Nb								9.93	9.71	8.32	7.91
Cs								0.32	0.34	0.24	0.27
Ba								908.0	915.4	322.3	315
La								52.95	50.99	15.87	16.02
Ce								103.2	99.7	33.03	33.76
Pr								11.45	11.61	4.21	4.28
Nd								43.30	41.97	17.69	17.34
Sm								6.79	6.69	3.68	3.66
Eu								1.79	1.79	1.16	1.17
Gd								4.74	5.01	3.34	3.15
Tb								0.60	0.64	0.51	0.53
Dy								3.26	3.10	2.84	2.84
Ho								0.69	0.66	0.57	0.57
Er								2.01	2.09	1.52	1.54
Tm								0.30	0.32	0.21	0.23
Yb								2.03	2.16	1.37	1.43
Lu								0.31	0.33	0.21	0.21
Hf								6.07	5.71	3.7	3.71
Ta								0.40	0.62	0.64	1.16
Th								11.23	11.44	2.64	2.61
U								0.90	0.90	0.89	0.92

Fe_2O_3t – total Fe; LOI – loss on ignition; Mg no. – $100^*(Mg^{2+}/(Mg^{2+}+Fe^{2+})$; R.V. – recommended value.

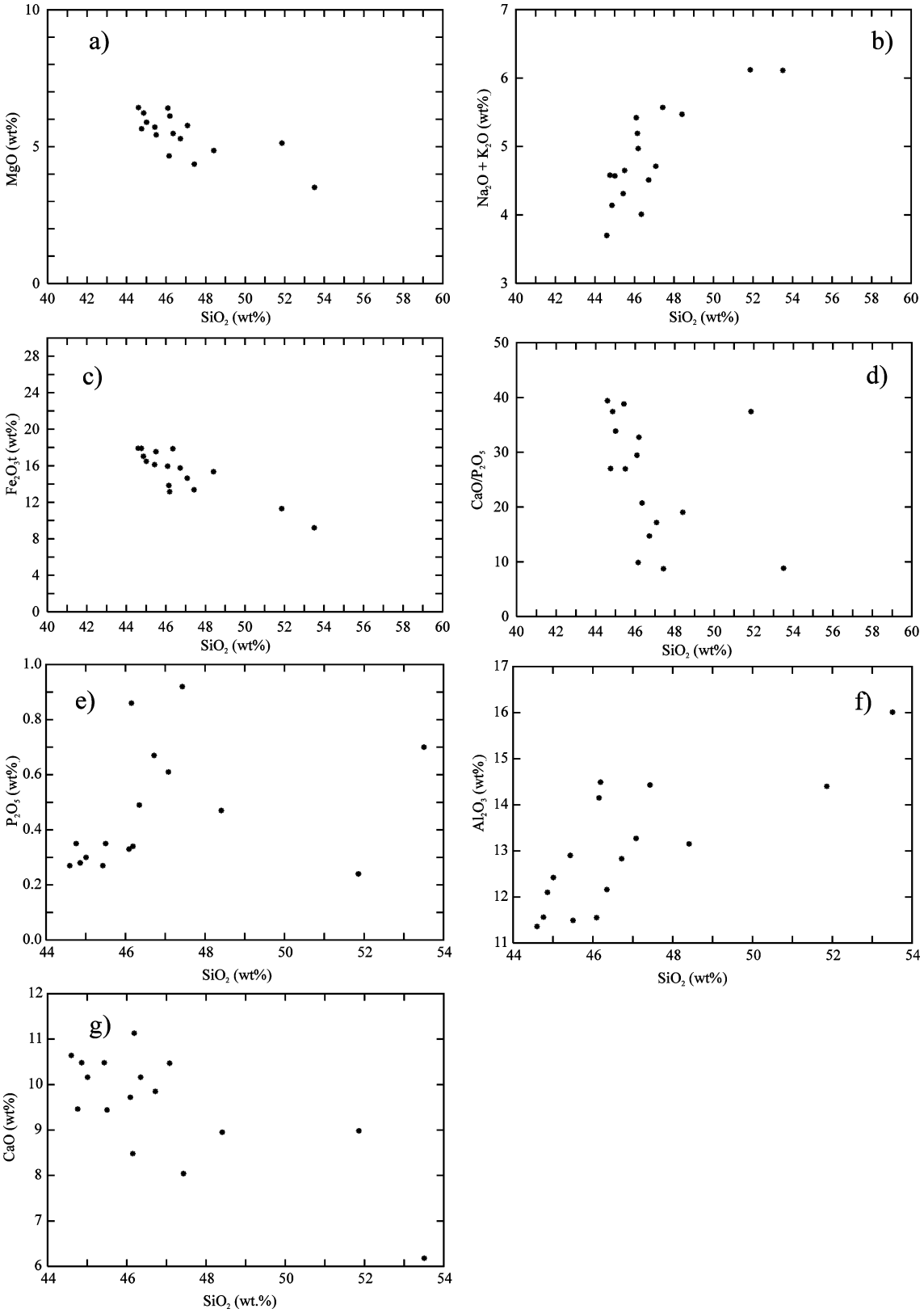

Figure 4. Major and trace element variations of the mafic dykes.

basalts. They have evolved Mg no. and low Ni content, and show chemical evolution trends which suggest they fractionated from a primitive magma. Their LREE-enriched patterns and incompatible trace element patterns are similar to the Emeishan flood basalts (Figs 6, 7) and their compositions also correspond to those of within-plate basalts and continental rift-related basalts on the

Table 3. Radiogenic isotope ratios and concentrations of Nd, Sm, Rb and Sr of a mafic dyke

Sample	Rb (ppm)	Sr (ppm)	$(^{87}Rb/^{86}Sr)_m$	$(^{87}Sr/^{86}Sr)_m$	$(^{87}Sr/^{86}Sr)_i$	Sm (ppm)	Nd (ppm)	$(^{147}Sm/^{144}Nd)_m$	$(^{143}Nd/^{144}Nd)_m$	$\varepsilon Nd_{(t)}$
GS04-025	40.0	360.5	0.3178	0.705640	0.704542	6.7	29.1	0.1396	0.512668	+2.7
GS04-028	53.7	406.9	0.3797	0.705867	0.704554	6.7	29.2	0.1388	0.512662	+2.6
BCR-1m	46.6	330	0.4045	0.705001		6.665	28.58	0.1412	0.512636	
BCR-1 r.v.				0.704960					0.512629	

$(^{87}Rb/^{86}Sr)_m$, $(^{87}Sr/^{86}Sr)_m$, $(^{147}Sm/^{144}Nd)_m$ and $(^{143}Nd/^{144}Nd)_m$ – measured isotopic ratios, respectively. $(^{87}Sr/^{86}Sr)_i$ and $\varepsilon Nd_{(t)}$ are calculated 242 Ma. Concentrations of Nd, Sm, Rb and Sr were determined by thermal ion mass spectrometer. BCR-1m – this study; BCR-1 r.v. – recommended value. All isotope values have 2σ of 14 or less.

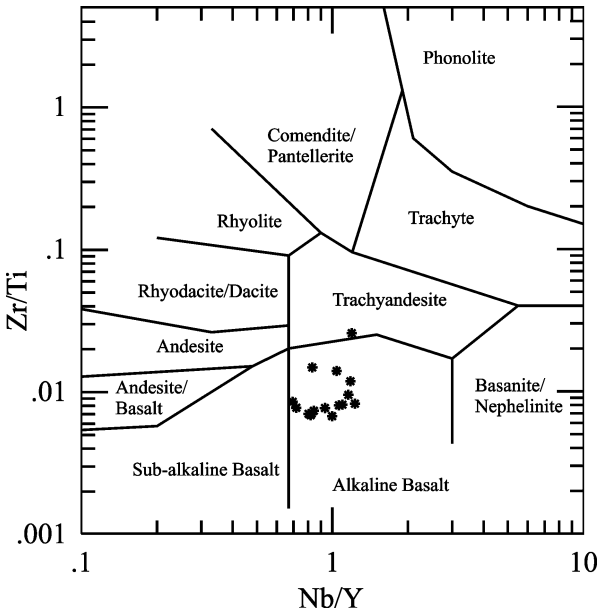

Figure 5. Trace element classification of the mafic alkaline dykes using the Zr/TiO_2 v. Nb/Y of Winchester & Floyd (1977).

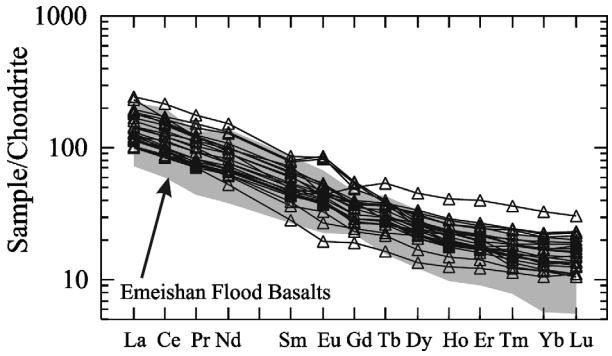

Figure 6. Chondrite-normalized rare-earth element data patterns of the mafic dykes and Emeishan flood basalts normalized to values of Sun & McDonough (1989). Flood basalt data from Song *et al.* (2001, 2004) and Xu *et al.* (2001).

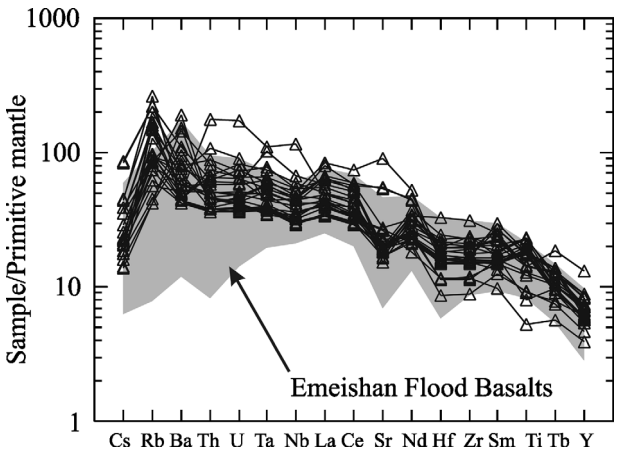

Figure 7. Primitive-mantle-normalized trace element data patterns plots of the mafic dykes and Emeishan flood basalts normalized to values of Sun & McDonough (1989). Flood basalt data from Song *et al.* (2001, 2004) and Xu *et al.* (2001).

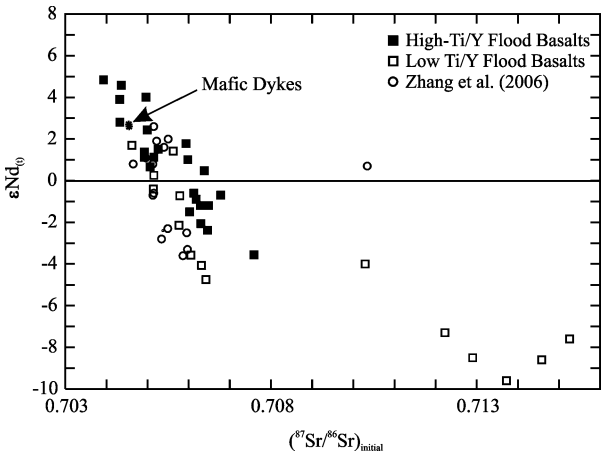

Figure 8. Sr–Nd isotope diagram showing the range of high-and low-Ti Emeishan Flood basalts and two mafic dykes (data from Song *et al.* 2001, 2004; Xu *et al.* 2001; Zhou *et al.* 2006 and Zhang *et al.* 2006).

tectonomagmatic discrimination diagram of Pearce & Cann (1973).

The positive $\varepsilon Nd_{(t)}$ values (+2.6 and +2.7) and low $(^{87}Sr/^{86}Sr)_i$ ratios suggest a mantle source which is consistent with basaltic and granitic rocks of the Panxi region (Xu *et al.* 2001; Shellnutt & Zhou, 2007) (Fig. 8). Many trace element ratios (Zr/Nb = 3.8–8.2, La/Nb = 0.4–1.7, Ba/La = 7.5–25.6) are consistent with an OIB-like source (Weaver, 1991; Song *et al.* 2001). This similarity leads us to conclude that the mafic dykes were also derived from the same plume-type source as the Emeishan flood basalts.

6.b. Magmatic history of the Emeishan large igneous province

Shellnutt & Zhou (2006) and Zhong *et al.* (2007) have reported ages of ~252 Ma. Identification of a ~242 Ma mafic dyke suggests another minor magmatic event in the Panxi region after the initial emplacement of the Emeishan flood basalts. We summarize the major magmatic periods of the Emeishan large igneous province and speculate on their causes.

6.b.1. ~260 Ma Emeishan large igneous province magmatism

The first reliable date for the Emeishan large igneous province was a U–Pb SHRIMP zircon date of 259 ± 3 Ma of a mafic intrusion in the Panxi region (Zhou *et al.* 2002*a*). Prior to the publication of this date, the age of the Emeishan large igneous province was thought to be Permo-Triassic and contemporaneous with the Siberian Traps (Chung & Jahn, 1995; Xu *et al.* 2001). During the last few years, numerous U–Pb SHRIMP dates of Emeishan large igneous province felsic and mafic intrusions have yielded ages around 260 Ma (Guo *et al.* 2004; Zhou *et al.* 2005, 2006; Luo *et al.* 2006; Zhong & Zhu, 2006; He *et al.* 2007; Shellnutt & Zhou, 2007; Zhong *et al.* 2007). The 260 Ma date is considered to be the eruption age for the Emeishan flood basalts because the compositions of mafic intrusions are similar to those of the flood basalts, and in many cases the plutonic rocks have intruded the lowermost Emeishan basalt flows, which suggests that the intrusions are nearly contemporaneous with volcanism. He *et al.* (2003) described the extent of erosion of the Maokou Formation (limestone) in southwest China and determined that the most extensive erosion was located in the west-central portion of the Emeishan large igneous province and decreased radially outward. The Maokou Formation was the last unit deposited prior to the eruption of the flood basalts and contains Late to Middle Permian fauna (He *et al.* 2003). They interpreted the differing erosion rates as a result of crustal doming caused by the arrival of a mantle plume. Xu *et al.* (2004) have also documented extensive geophysical features of the crust beneath the Emeishan large igneous province, which they interpret to represent the fossil Emeishan plume-head. The varying thickness of the seismically defined layers documented by Xu *et al.* (2004) corresponds with the surface erosion zones of He *et al.* (2003). He *et al.* (2007) also have dated a volcanic ash layer just above the Emeishan flood basalts at ~260 Ma, which they have interpreted to represent the termination age. Many of the published dates are from the Panxi region with a few from the eastern margin of the Emeishan large igneous province. The location of the dated rocks is important because the Panxi region is located in the inner zone (centre) of the crustal doming model and therefore would represent the oldest portion of the Emeishan large igneous province. The fact that 260 Ma ages are also found in the eastern margin of the Emeishan large igneous province suggests that a relatively uniform and rapid emplacement occurred.

6.b.2. ~252 Ma magmatism

In contrast to the plutonic rocks, the Emeishan flood basalts have consistently yielded younger ages, between 251 Ma and 255 Ma, using ^{40}Ar–^{39}Ar methods (Boven *et al.* 2002; Lo *et al.* 2002; Fan *et al.* 2004). There have been a few U–Pb dates for acidic ash layers in southwestern China which correspond to the Permo-Triassic boundary, however, no flood basalts have been dated using this method (Chung & Jahn, 1995; Bowring *et al.* 1998; Gradstein, Ogg & Smith, 2005). Fan *et al.* (2004) proposed a model in which Emeishan large igneous province magmatism began at ~260 Ma with the emplacement of some mafic intrusions, followed by eruption of the flood basalts within a short period around ~255 Ma and ending between 251 and 253 Ma. The implication is that Emeishan large igneous province magmatism spanned the Late Permian and contributed to two separate mass extinctions, the end-Guadalupian (260 Ma) and Permo-Triassic (251 Ma), and may have been synchronous with the much more voluminous Siberian Traps magmatism (Lo *et al.* 2002; Fan *et al.* 2004; Gradstein, Ogg & Smith, 2005). Two plutons in the Panxi region, the Huangcao and Ailanghe plutons, have yielded SHRIMP zircon ages of 252 ± 2.5 and 251 ± 6 Ma, respectively (Shellnutt & Zhou, 2006; Zhong *et al.* 2007). This is the first evidence from the plutonic rocks that Emeishan magmatism may have extended to the Late Permian.

Palaeomagnetic, geological and geochronological evidence suggests that volcanism was not likely to have extended far beyond ~260 Ma because the flood basalts erupted within one normal-polarity episode and there is no evidence of weathered flow tops indicating rapid eruption rates (Huang & Opdyke, 1998; Thompson *et al.* 2001; Ali *et al.* 2005; He *et al.* 2007). The ages of the Huangcao and Ailanghe plutons are the only U–Pb ages of ~252 Ma, however, the results of Zhong *et al.* (2007) have a large error (± 6 Ma). These two plutons are volumetrically insignificant when compared to the volume of the flood basalts and likely represent a different stage of post-flood basalt magmatism because the sources of the two plutons are different, with the Huangcao pluton being mantle derived ($\varepsilon Nd_{(t)} = +1.3$ to $+1.9$) and the Ailanghe pluton being crustally derived (Shellnutt & Zhou, 2007; Zhong *et al.* 2007).

The U–Pb ages from acidic ash flow layers that define the Permian–Triassic boundary in southwestern China are definitive evidence for Permo-Triassic volcanism in this region (Bowring *et al.* 1998; Fan *et al.* 2004). However, widespread volcanism at this time is well

known throughout southwest China and Eurasia in general, but whether or not Emeishan large igneous province magmatism is responsible for those layers remains to be confirmed (Yin *et al.* 1992).

6.b.3. ∼ 242 Ma magmatism

The age of the mafic dyke at ∼ 242 Ma is the first reported Early–Middle Triassic age for mafic igneous rocks in the Panxi region (Gradstein, Ogg & Smith, 2005). Zircons retrieved from the Huangcao pluton, intruded by mafic dykes of similar composition, revealed a bimodal distribution of ages at 240 Ma and 252 Ma, respectively (Shellnutt & Zhou, 2006). The presence of the 240 Ma zircons in the Huangcao pluton may be the result of contamination from the dykes. The Rb–Sr isotopic data from the Huangcao pluton yield an isochron age of ∼ 248 Ma, which is close to the ∼ 252 Ma interpreted age. The implication is that the ∼ 240 Ma zircon results from the Huangcao pluton may have originated from the dykes.

6.c. Possible mechanisms for post-260 Ma melting events

There are at least two, volumetrically minor, post-260 Ma magmatic events in the Yangtze Block. It is unclear why there were periods of mafic magmatism after the main effusive period of the Emeishan large igneous province, however, we suggest that the fossil plume-head as documented by Xu *et al.* (2004) was the ultimate source of the ∼ 252 Ma Huangcao pluton and the ∼ 242 Ma mafic dykes. Although the same mantle source was melted, they were distinct melting events under different conditions. Technically, this would not represent melting associated with the Emeishan large igneous province plume, merely melting of fossil plume-head material. Shellnutt & Zhou (2007) have suggested that post-ELIP relaxation of the Yangtze crust was likely responsible for melting underplated mafic rocks emplaced at ∼ 260 Ma and likely melted the crust as well, and caused the formation of the Ailanghe pluton at 251 ± 6 Ma (Zhong *et al.* 2007).

The dykes are spatially associated with the flood basalts but their relationship to them is not known. The dykes suggest that either the Emeishan mantle-plume was continually active and produced flood basalts for 18 Ma, or that another period of melting unrelated to the flood basalt magmatism occurred. The fact that the dykes were formed by extensional processes suggests that they could be related to the Emeishan large igneous province but why did the mafic dykes form so late (cf. Fahrig, 1987; Pollard, 1987)?

Regional tectonic studies of South China–Indochina indicate there was a major tectonothermal event during Late Permian and Middle Triassic times (Nam *et al.* 2001; Lepvrier *et al.* 2004; Yan *et al.* 2006). The cause of the tectonothermal event is thought to be the collision between the South China and Indochina blocks (Fig. 9). Afterward, northward subduction of an amalgamated South China–Indochina block collided with the North China block at ∼ 230 Ma (Lan *et al.* 2000; Lepvrier *et al.* 2004; Liu *et al.* 2006; Yan *et al.* 2006). The mafic dykes are older than the collision between North China and the South China–Indochina block but younger than the South China–Indochina collision. The age of 242 Ma indicates that extension-related magmatism must have occurred within the western margin of the South China–Indochina Block just prior to final suturing of the North China and South China–Indochina blocks (Fig. 9).

6.d. Duration of the Emeishan large igneous province magmatism

Mantle plumes and hotspot magmatism have been known to be continuously active for long periods of time, but ∼ 18 Ma between the eruptions of the first basalts and dyke injection is on the high side for the duration of mantle plume-derived continental large igneous provinces (Abbott & Isley, 2002). Long-lived hotspot and mantle plume magmatism is common in the ocean basins and is responsible for the formation of ocean-island/seamount chains and oceanic plateaux (e.g. Morgan, 1972; Richards, Duncan & Courtillot, 1989). A long chain of ocean islands and seamounts across the central Pacific leading back to an active hotspot, for example, Hawaii, is intuitive evidence of a long eruptive history (Wilson, 1965). It is difficult to assess intuitively the duration of mantle plume-derived continental large igneous provinces because the time-dependent geological evidence (e.g. hotspot track) is usually absent or there is a complex magmatic history. Instead, the duration of continental large igneous provinces is largely determined by dating techniques, although some geological relationships can be used (e.g. absence of sedimentary layers between lava flows). Many continental large igneous provinces are thought to erupt with variable time spans but generally within 10 million years with peak volcanic activity lasting less than a few million years (e.g. Coffin & Eldholm, 1994; Abbott & Isley, 2002; Ernst, Buchan & Campbell, 2005). Age dates by Shellnutt & Zhou (2006) and Zhong *et al.* (2007) have confirmed that magmatism occurred 8 to 9 million years after the main effusive period of the Emeishan large igneous province, and now an age date from a mafic dyke confirms that compositionally similar mafic magmatism occurred even later. At least three periods of magmatism in southwestern China can be identified and likely correspond to the melting of the Emeishan mantle plume at ∼ 260 Ma and further remelting of the fossil plume head at ∼ 252 Ma and ∼ 242 Ma. This does not imply that Emeishan magmatism was a continuous process, although it is possible, only that the plume-head served as a source for a diverse set of magmas for ∼ 18 million years and possibly longer.

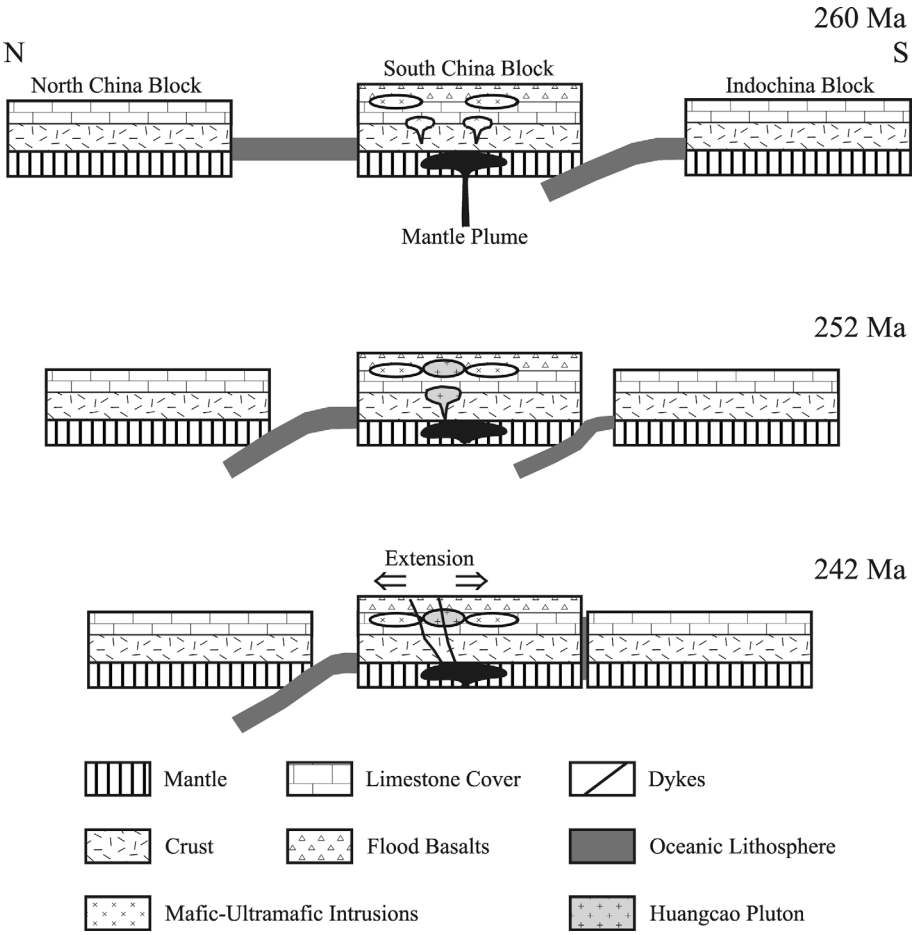

Figure 9. A simplified model summarizing the three magmatic periods involving the ELIP mantle plume-head and the relative locations of the North China block and Indochina block to the South China block. At 260 Ma the flood basalts and layered mafic–ultramafic intrusions are emplaced. At 252 Ma, extension-related magmatism causes remelting of the ELIP mantle plume head and also melting of the Yangtze basement rocks. Collision between North China and South China causes a volumetrically minor melting of the fossil plume-head.

The precise duration of Emeishan flood basalt volcanism remains unknown. Huang & Opdyke (1998), Thompson *et al.* (2001) and He *et al.* (2003, 2007) suggested that volcanism and doming were short-lived, probably within one magnetic reversal cycle, or less than 1 million years (Ali *et al.* 2005). This interpretation is consistent with estimated eruption rates and emplacement models for many large igneous provinces (e.g. Coffin & Eldholm, 1994). Radiometric dates of Permo-Triassic ($\sim$ 251 Ma) mafic and acidic layers in SW China may be correlative with the Emeishan large igneous province, however, it is not confirmed (Fan *et al.* 2004; Kamo, Crowley & Bowring, 2006).

7. Conclusions

There have been at least two post-260 Ma magmatic events in the Yangtze Block in which the magmatic rocks have geochemical characteristics similar to the Emeishan flood basalts. Magmatism at 252 Ma produced at least two small felsic plutons. The plutonic rocks were likely generated by melting of the Yangtze basement and underplated mafic magmas of the Emeishan large igneous province due to post-emplacement relaxation of the Yangtze crust. The second melting event at $\sim$ 242 Ma occurred $\sim$ 10 million years after formation of the felsic plutons and produced the mafic alkaline dykes in the Panxi region of the Emeishan large igneous province. The dykes indicate that there was extension-related magmatism prior to the collision between the South China and North China blocks.

Acknowledgements. We thank Andy Saunders and John Mahoney for their constructive reviews of our manuscript. We also thank Professor Ma Yuxiao and Mr Zhao Hao, both from Chengdu University of Science and Technology, for their field support, and Dr Liang Qi and Mrs Xiao Fu for their analytical support at the University of Hong Kong. This study is supported by grants from the Research Grant Council of Hong Kong, SAR (HKU7057/05P) and the Chinese 111 Project B07011.

References

ABBOTT, D. H. & ISLEY, A. E. 2002. The intensity, occurrence, and duration of superplume events and eras over geological time. *Journal of Geodynamics* **34**, 265–307.

ALI, J. R., LO, C.-H., THOMPSON, G. M. & SONG, X. Y. 2004. Emeishan basalt Ar–Ar overprint ages define several tectonic events that affected the western Yangtze platform in the Mesozoic Cenozoic. *Journal of Asian Earth Science* **23**, 163–78.

ALI, J. R., THOMPSON, G. M., ZHOU, M.-F. & SONG, X. Y. 2005. Emeishan large igneous province, SW China. *Lithos* **79**, 475–89.

BEGEMANN, F., LUDWIG, K. R., LUGMAIR, G. W., MIN, K., NYQUIST, L. E., PATCHETT, P. J., RENNE, P. R., SHIH, C.-Y., VILLA, I. M. & WALKER, R. J. 2001. Call for an improved set of decay constants for geochronological use. *Geochimica et Cosmochimica Acta* **65**, 111–21.

BLACK, L. P., KAMO, S. L., ALLEN, C. M., ALEINIKOFF, J. N., DAVIS, D. W., KORSCH, R. J. & FOUDOULIS, C. 2003*a*. TEMORA 1: a new zircon standard for Phanerozoic U–Pb geochronology. *Chemical Geology* **200**, 155–70.

BLACK, L. P., KAMO, S. L., WILLIAMS, I. S., MUNDIL, R., DAVIS, D. W., KORSCH, R. J. & FOUDOULIS, C. 2003*b*. The application of SHRIMP to Phanerozoic geochronology; a critical appraisal of four zircon standards. *Chemical Geology* **200**, 171–88.

BOVEN, A., PASTEELS, P., PUNZALAN, L. E., LIU, J., LUO, X., ZHANG, W., GUO, Z. & HERTOGEN, J. 2002. $^{40}Ar/^{39}Ar$ geochronological constraints on the age and evolution of the Permo-Triassic Emeishan volcanic province, southwest China. *Journal of Asian Earth Sciences* **20**, 157–75.

BOWRING, S. A., ERWIN, D. H., JIN, Y. G., MARTIN, M. W., DAVIDEK, K. & WANG, W. 1998. U/Pb Zircon geochronology and tempo of the end-Permian mass extinction. *Science* **280**, 1039–45.

BRUGUIER, O., LANCELOT, J. R. & MALAVIEILLE, J. 1997. U–Pb dating on single detrital zircon grains from the Triassic Songpan–Ganze flysch Central China: provenance and tectonic correlations. *Earth and Planetary Science Letters* **152**, 217–31.

CAMPBELL, I. H. & GRIFFITHS, R. W. 1990. Implications of mantle plume structure for the evolution of flood basalts. *Earth and Planetary Science Letters* **99**, 79–93.

CARTER, A., ROQUES, D., BRISTOW, C. & KINNY, P. 2001. Understanding Mesozoic accretion in southeast Asia: significance of Triassic thermotectonism (Indosinian orogeny) in Vietnam. *Geology* **29**, 211–14.

CHEN, F., HEGNER, E. & TODT, W. 2000. Zircon ages, Nd isotopic and chemical compositions of orthogneisses from the Black Forest, Germany – evidence for a Cambrian magmatic arc. *International Journal of Earth Sciences* **88**, 791–802.

CHEN, F., SIEBEL, W., SATIR, M., TERZIOGLU, N. & SAKA, K. 2002. Geochronology of the Karadere basement (NW Turkey) and implications for the geological evolution of the Istanbul zone. *International Journal of Earth Sciences* **91**, 469–81.

CHUNG, S. L. & JAHN, B.-M. 1995. Plume–lithosphere interaction in generation of the Emeishan flood basalts at the Permian–Triassic boundary. *Geology* **23**, 889–92.

CHUNG, S. L., JAHN, B.-M., GENYAO, W., LO, C. H. & BOLIN, C. 1998. The Emeishan flood basalt in SW China: a mantle plume initiation model and its connection with continental breakup and mass extinction at the Permian–Triassic boundary. In *Mantle Dynamics and Plate Interactions in East Asia* (eds M. F. J. Flower, S.-L. Chung, C. H. Lo & T. Y. Lee), pp. 47–58. American Geophysical Union, Geodynamic Series Volume 27.

CLAOUÉ-LONG, J. C., COMPSTON, W., ROBERTS, J. & FANNING, M. 1995. Two Carboniferous ages: a comparison of SHRIMP zircon dating with conventional zircon ages and $^{40}Ar/^{39}Ar$ analysis. In *Geochronology Time Scales and Global Stratigraphic Correlation* (eds W. A. Berggren, D. V. Kent, M. P. Aubrey & J. Hardenbol), pp. 3–21. SEPM Special Publication no. 54.

COFFIN, M. F. & ELDHOLM, O. 1994. Large igneous provinces: crustal structure, dimensions and external consequences. *Reviews of Geophysics* **32**, 1–36.

COMPSTON, W., WILLIAMS, I. S. & MEYER, C. 1984. U–Pb geochronology of zircons from Lunar breccia 73217 using a sensitive high mass-resolution ion microprobe. *Journal of Geophysical Research* **89**, 525–34.

COURTILLOT, V., JAUPART, C., MANIGHETTI, I., TAPPONNIER, P. & BESSE, J. 1999. On causal links between flood basalts and continental break-up. *Earth and Planetary Science Letters* **166**, 177–95.

ERNST, R. E., BUCHAN, K. L. & CAMPBELL, I. H. 2005. Frontiers in large igneous province research. *Lithos* **79**, 271–97.

FAHRIG, W. F. 1987. The tectonic settings of continental mafic dyke swarms: failed arm and early passive margin. In *Mafic Dyke Swarms* (eds H. C. Halls & W. F. Fahrig), pp. 331–48. Geological Association of Canada, Special Paper no. 34.

FAN, W., WANG, V., PENG, T., MIAO, L. & GUO, F. 2004. Ar–Ar and U–Pb geochronology of late Paleozoic basalts in western Guangxi and its constraints on the eruption age of Emeishan basalt magmatism. *Chinese Science Bulletin* **49**, 2318–27.

Gill, R. (ed.) 1997. *Modern Analytical Geochemistry: an introduction to quantitative chemical analysis for earth, environment and materials scientists*. Singapore: Addison Wesley Longman, 329 pp.

GRADSTEIN, F. M., OGG, J. G. & SMITH, A. G. (eds) 2005. *A geologic time scale 2004*. Cambridge: Cambridge University Press, 589 pp.

GUO, F., FAN, W., WANG, Y. & LI, C. 2004. When did the Emeishan mantle plume activity start? Geochronological and geochemical evidence from ultramafic–mafic dikes in southwestern China. *International Geology Review* **46**, 226–34.

HALLS, H. C. 1982. The importance and potential of mafic dyke swarms in studies of geodynamic processes. *Geoscience Canada* **9**, 145–54.

HE, B., XU, Y.-G., CHUNG, S.-L., XIAO, L. & WANG, Y. 2003. Sedimentary evidence for a rapid, kilometer-scale crustal doming prior to the eruption of the Emeishan flood basalts. *Earth and Planetary Science Letters* **213**, 391–405.

HE, B., XU, Y.-G., HUANG, X.-L., LUO, Z.-Y., SHI, Y.-R., YANG, O.-J. & YU, S.-Y. 2007. Age and duration of the Emeishan flood volcanism, SW China: Geochemistry and SHRIMP zircon U–Pb dating of silicic ignimbrites, post-volcanic Xuanwei Formation and clay tuff at the Chaotian section. *Earth and Planetary Science Letters* **255**, 306–23.

HOOPER, P. R. 1997. The Columbia River flood basalt province: current status. In *Large Igneous Provinces: Continental, Oceanic, and Planetary Flood Volcanism*

(eds J. J. Mahoney & M. F. Coffin.), pp. 1–27. American Geophysical Union, Geophysical Monograph Series no. 100.

HUANG, K. & OPDYKE, N. D. 1998. Magnetostratigraphic investigations of an Emeishan basalt section in western Guizhou Province, China. *Earth and Planetary Science Letters* **163**, 1–14.

KAMO, S. L., CROWLEY, J. & BOWRING, S. A. 2006. The Permian–Triassic boundary event and eruption of the Siberian flood basalts: An inter-laboratory U–Pb dating study. *Geochimica et Cosmochimica Acta* **70**, A303.

LAN, C.-Y., CHUNG, S.-L., SHEN, J.-S., LO, C.-H., WANG, P.-L., HOA, T. T., THANH, H. H. & MERTZMAN, S. A. 2000. Geochemical and Sr–Nd isotopic characteristics of granitic rocks from northern Vietnam. *Journal of Asian Earth Sciences* **18**, 267–80.

LEPVRIER, C., MALUSKI, H., TICH, V. V., LEYRELOUP, A., THI, P. T. & VUONG, N. V. 2004. The early Triassic Indosinian orogeny in Vietnam (Truong Son Belt and Kontum Massif); implications for the geodynamic evolution of Indochina. *Tectonophysics* **393**, 87–118.

LI, S. G., XIAO, Y. L., LIOU, D. L., CHEN, Y. Z., GE, N. J., ZHANG, Z. Q., SUN, S. S., CONG, B. L., ZHANG, R. Y., HART, S. R. & WANG, S. S. 1993. Collision of the north China and Yangtse blocks and formation of coesite-bearing eclogites – timing and processes. *Chemical Geology* **109**, 89–111.

LI, Z. X., ZHANG, L. & POWELL, C. M. 1995. South China in Rodinia: part of the missing link between Australia–East Antarctica and Laurentia. *Geology* **23**, 407–10.

LIU, D., JIAN, P., KRÖNER, A. & XU, S. 2006. Dating of prograde metamorphic events deciphered from episodic zircon growth in rocks of the Dabie–Sulu UHP complex, China. *Earth and Planetary Science Letters* **250**, 650–66.

LO, C. H., CHUNG, S.-L., LEE, T.-Y. & WU, G. 2002. Age of the Emeishan flood magmatism and relations to Permian–Triassic boundary events. *Earth and Planetary Science Letters* **198**, 449–58.

LUDWIG, K. R. 2001. *Isoplot/Ex, rev. 2.49: A Geochronological Toolkit for Microsoft Excel*. Berkeley Geochronological Center, Special Publication no. 1a, 58 pp.

LUO, Z.-Y., XU, Y.-G., HE, B., HUANG, X.-L. & SHI, Y. R. 2006. A-type granite and syenite intrusions in Emeishan large igneous provinces: product of the Emeishan plume? *International Conference on Continental Volcanism IAVCEI2006 Abstracts & Program*, p. 63.

MENG, Q.-R. & ZHANG, G.-W. 1999. Timing of collision of the north and south China blocks: controversy and reconciliation. *Geology* **27**, 123–6.

METCALFE, I. 2006. Palaeozoic and Mesozoic tectonic evolution and palaeogeography of east Asian crustal fragments: the Korean peninsula in context. *Gondwana Research* **9**, 24–46.

MORGAN, W. J. 1972. Deep mantle convection plumes and plate motions. *American Association of Petroleum Geologists Bulletin* **56**, 203–13.

NAM, T. N. 1998. Thermotectonic events from Early Proterozoic to Miocene in the Indochina craton: implication of K–Ar ages in Vietnam. *Journal of Asian Earth Sciences* **16**, 475–84.

NAM, T. N., SANO, Y., TERADA, K., TORIUMI, M., QUYNH, P. V. & DUNG, L. T. 2001. First SHRIMP U–Pb zircon dating of granulites from the Kontum massif (Vietnam) and tectonothermal implications. *Journal of Asian Earth Sciences* **19**, 77–84.

PEARCE, J. A. & CANN, J. R. 1973. Tectonic setting of basic volcanic rocks determined using trace element analyses. *Earth and Planetary Science Letters* **19**, 290–300.

POLLARD, D. D. 1987. Elementary fracture mechanics applied to the structural interpretation of dykes. In *Mafic Dyke Swarms* (eds H. C. Halls & W. F. Fahrig.), pp. 5–24. Geological Association of Canada, Special Paper no. 34.

POTTS, P. J., THOMPSON, M., KANE, J. S. & PETROV, L. L. 2000. GEOPT7. An international proficiency test for analytical geochemistry laboratories. Report on Round 7. *Geostandards Newsletter*, 35 pp.

POTTS, P. J., THOMPSON, M., WEBB, P. C. & WATSON, J. S. 2001. GEOPT9. An international proficiency test for analytical geochemistry laboratories. Report on Round 9. *Geostandards Newsletter*, 36 pp.

QI, L., JING, H. & GREGOIRE, D. C. 2000. Determination of trace elements in granites by inductively coupled plasma mass spectrometry. *Talanta* **51**, 507–13.

RACZEK, I., JOCHUM, K. L. & HOFMANN, A. W. 2003. Neodymium and strontium isotope data for USGS reference materials BCR-1, BCR-2, BHVO-1, BHVO-2, AGV-1, AGV-2, GSP-1, GSP-2 and eight MPI-DING reference glasses. *Geostandards Newsletter* **27**, 173–9.

RICHARDS, M., DUNCAN, R. A. & COURTILLOT, V. E. 1989. Flood basalts and hotspot tracks: plumes heads and tails. *Science* **246**, 103–7.

SHELLNUTT, J. G. & ZHOU, M.-F. 2006. Rifting-related, Permian ferrosyenites in the Panxi region of the Emeishan large Igneous province, SW China. *Geochimica et Cosmochimica Acta* **70**, A579.

SHELLNUTT, J. G. & ZHOU, M.-F. 2007. Permian peralkaline, peraluminous and metaluminous A-type granites in the Panxi district, SW China: their relationship to the Emeishan mantle plume. *Chemical Geology* **243**, 286–316.

SONG, X.-Y., ZHOU, M.-F., CAO, Z.-M. & ROBINSON, P. 2004. Late Permian rifting of the South China craton caused by the Emeishan mantle plume? *Journal of Geological Society, London* **161**, 773–81.

SONG, X. Y., ZHOU, M.-F., HOU, Z.-Q., CAO, Z.-M., WANG, Y.-L. & LI, Y. 2001. Geochemical constraints on the mantle source of the upper Permian Emeishan continental flood basalts, southwestern China. *International Geology Review* **43**, 213–25.

SUN, S. S. & MCDONOUGH, W. F. 1989. Chemical and isotopic systematics of oceanic basalts: implications for mantle composition and processes. In *Magmatism in the Ocean Basins* (eds A. D. Saunders & M. J. Norry.), pp. 313–45. Geological Society of London, Special Publication no. 42

THOMPSON, G. M., ALI, J. R., SONG, X. Y. & JOLLEY, D. W. 2001. Emeishan basalts, southwest China: reappraisal of the formation's type area stratigraphy and a discussion of its significance as a large igneous province. *Journal of the Geological Society, London* **158**, 593–9.

THOMPSON, M., POTTS, P. J., KANE, J. S. & WILSON, S. 1999. GEOPT5. An international proficiency test for analytical geochemistry laboratories. Report on Round 5. *Geostandards Newsletter*, 23 pp.

WANG, D. R., XIE, Y. M., WANG, Q. J. & TAO, Z. D. 1994. *Geology of Guabang area (Map G-48-25-C)*. Panxi Geological Team, Geology and Mineral Resources Bureau, Sichuan Province, 1:50000.

WEAVER, B. L. 1991. The origin of ocean island basalt end-member compositions: trace element and isotopic constraints. *Earth and Planetary Science Letters* **104**, 381–97.

WHITE, R. S. & MCKENZIE, D. 1989. Magmatism at rift zones: the generation of volcanics continental margins and flood basalts. *Journal of Geophysical Research* **94**, 7685–729.

WHITE, R. S. & MCKENZIE, D. 1995. Mantle plumes and flood basalts. *Journal of Geophysical Research* **100**, 543–85.

WILSON, J. T. 1965. Evidence from ocean islands suggesting movement in the Earth. *Royal Society of London Philosophical Transactions* **A258**, 145–67.

WINCHESTER, J. A. & FLOYD, P. A. 1977. Geochemical discrimination of different magma series and their differentiation products using immobile elements. *Chemical Geology* **20**, 325–43.

XIONG, X. Y., XIE, Y. M., NIE, K. H., KAN, Z. Z., DING, L. R. & GUO, J. Q. 1996. *Geology of Miyi area (Map G-48-37-A)*. Panxi Geological Team, Geology and Mineral Resources Bureau, Sichuan Province, 1:50000.

XU, Y., CHUNG, S.-L., JAHN, B.-M. & WU, G. 2001. Petrologic and geochemical constraints on the petrogenesis of Permian–Triassic Emeishan flood basalts in southwestern China. *Lithos* **58**, 145–68.

XU, Y.-G., HE, B., CHUNG, S.-L., MENZIES, M. & FREY, F. A. 2004. Geologic, geochemical, and geophysical consequences of plume involvement in the Emeishan flood-basalt province. *Geology* **32**, 917–20.

YAN, D.-P., ZHOU, M.-F., SONG, H. L. & FU, Z. R. 2003*a*. Structural style and tectonic significance of the Jianglang tectonic dome, eastern margin of the Tibetan Plateau, China. *Journal of Structural Geology* **25**, 765–79.

YAN, D.-P., ZHOU, M.-F., SONG, H. L., WANG, X. W. & MALPAS, J. 2003*b*. Origin and tectonic significance of a Mesozoic multi-layer over-thrust system within the Yangtze Block (South China). *Tectonophysics* **361**, 239–54.

YAN, D.-P., ZHOU, M.-F., WANG, C. Y. & XIA, B. 2006. Structural and geochronological constraints on the tectonic evolution of the Dulong-Song Chay tectonic dome in Yunnan province, SW China. *Journal of Asian Earth Sciences* **28**, 332–53.

YIN, H., HUANG, X., ZHANG, K., HANSEN, H. J., YANG, F., DING, M. & BIE, X. 1992. The effects of volcanism of the Permo-Triassic mass extinction in South China. In *Permo-Triassic Events in the Eastern Tethys: Stratigraphy, Classification, and Relations with the Western Tethys* (eds W. C. Sweet, Z. Y. Yang, J. M. Dickins & H. F. Yin.), pp. 146–57. *World and Regional Geology* **2**.

ZHANG, Z., MAHONEY, J. J., MAO, J. & WANG, F. 2006. Geochemistry of Picritic and Associated Basalt Flows of the Western Emeishan Flood Basalt Province, China. *Journal of Petrology* **47**, 1997–2019.

ZHONG, H., ZHOU, X. H., ZHOU, M.-F., SUN, M. & LIU, B. G. 2002. Platinum-group element geochemistry of the Hongge Fe–V–Ti deposit in the Pan-Xi area, southwestern China. *Mineralium Deposita* **37**, 226–39.

ZHONG, H. & ZHU, W.-G. 2006. Geochronology of layered mafic intrusions from the Panxi area in the Emeishan large igneous province, SW China. *Mineralium Deposita* **41**, 599–606.

ZHONG, H., ZHU, W.-G., SONG, X. Y. & HE, D.-F. 2007. SHRIMP U–Pb zircon geochronology, geochemistry, and Nd–Sr isotopic study of contrasting granites in the Emeishan large igneous province, SW China. *Chemical Geology* **236**, 112–37.

ZHOU, M.-F., MALPAS, J., SONG, X. Y., ROBINSON, P. T., SUN, M., KENNEDY, A. K., LESHER, C. M. & KEAYS, R. R. 2002*a*. A temporal link between the Emeishan large igneous province (SW China) and the end-Guadalupian mass extinction. *Earth and Planetary Science Letters* **196**, 113–22.

ZHOU, M.-F., ROBINSON, P. T., LESHER, C. M., KEAYS, R. R., ZHANG, C. J. & MALPAS, J. 2005. Geochemistry, petrogenesis and metallogenesis of the Panzhihua gabbroic layered intrusion and associated Fe–Ti–V oxide deposits, Sichuan Province, SW China. *Journal of Petrology* **46**, 2253–80.

ZHOU, M.-F., YAN, D.-P., KENNEDY, A. K., LI, Y. & DING, J. 2002*b*. SHRIMP U–Pb zircon geochronological and geochemical evidence for Neoproterozoic arc-magmatism along the western margin of the Yangtze block, South China. *Earth and Planetary Science Letters* **196**, 51–67.

ZHOU, M.-F., ZHAO, J.-H., QI, L., SU, W. & HU, R. Z. 2006. Zircon U–Pb geochronology and elemental and Sr–Nd isotopic geochemistry of Permian mafic rocks in the Funing area, SW China. *Contributions to Mineralogy and Petrology* **151**, 1–19.